PHILIPPINE ENGINEERING JOURNAL
PEJ 2014; Vol. 35, No. 1: 53-63

SIMULATION OF SHOCK WAVES IN SUPERSONIC FLOW OF CO_2 THROUGH A CONVERGING-DIVERGING NOZZLE OF TRANSCRITICAL EJECTOR REFRIGERATION SYSTEM

Menandro Serrano Berana[a] and Masafumi Nakagawa[b]

[a]*Mechanical Engineering Department, University of the Philippines-Diliman, Quezon City, 1101 Philippines, menandro.berana@coe.upd.edu.ph*

[b]*Mechanical Engineering Department, Toyohashi University of Technology, Toyohashi City Aichi, 441-8580, Japan ,nakagawa@mech.tut.ac.jp*

ABSTRACT

Shock waves in non-equilibrium liquid-vapor flow in a converging-diverging nozzle were simulated and compared to the experimental results in previous studies of the authors. Additional findings from simulation in the present study were found to be in agreement with the experimental results.

In the simulation, flow of uniformity dispersed droplets and vapor was assumed. Momentum and thermal relaxation phenomena were incorporated in the derived equations. Simulation results using the equations for supersonic two-phase flow of CO_2 in converging-diverging nozzles intended for a research on the transcritical ejector refrigeration system are presented.

In a first previous study by the authors, shock waves along the diverging sections of relatively long nozzles were investigated in a blowdown device. Inlet conditions near the critical point were selected, wherein the pressure range was 8-9 MPa and the obtained temperature range was 25-41°C. Correspondingly, back pressures ranged from 1.2 to 4.2 MPa. In a second study by the authors, the expansion valve of the vapor compression refrigeration used was replaced by a relatively short converging-diverging nozzle to isolate the nozzle and to easily investigate its inlet and outlet states. The inlet conditions used were 9-11 MPa at 37-55°C. To determine different intensities of shock waves, the widest possible back-pressure range obtained was 3.6-5.9 MPa.

Relaxation phenomena, weak pseudo-shock waves occurred in liquid-dominated two-phase flow, while dispersed shock waves occurred in vapor-dominated flow. It was simulated and verified in this study that shock waves intensify with increasing divergence angle given the same inlet condition, and with increasing supercritical inlet entropy given the same nozzle. The results are in agreement with the experiment and similar simulation results in the previous studies.

The nonequilibrium two-phase flow model can be used in analyzing flow in nozzles and other components of ejector refrigeration systems and designing an ejector.

Correspondence to: Menandro S. Berana, University of the Philippines, Diliman, Quezon City 1101, Philippines, email: *menandro.berana@coe.udp.edu.ph*

Received: February 4, 2013
Accepted: April 1, 2014

1. INTRODUCTION

Researches, technological innovations, balanced utilization of natural resources and implementation of well-reviewed policies are being carried out worldwide to prevent global warming and ozone depletion, preserve the ecosystem and reduce costs. Refrigeration and air conditioning are among the technologies that have become indispensible to humanity. People continuously improve their quality of living with the help of such technologies. Improvement and breakthroughs in this field are being sought not only for the benefit of the people but also for the preservation of the environment.

CO_2 is a safe working fluid and benign to the environment that has been widely investigated for and used in ejector refrigeration systems.

Refrigerants may undergo single phase and two-phase flow processes, and shock waves can occur in any of such flows. Shock waves can degrade the performance of a refrigeration cycle by lowering the kinetic energy of supposedly accelerating flow and thus the coefficient or performance of the cycle is reduced. Specifically, they significantly decrease the energy-conversion efficiency of converging-diverging nozzles of ejector refrigeration systems. Therefore, shock waves should be investigated so that optimum nozzle design can be attained by avoiding them. This in turn can lead to closely achieving the designed energy conversion efficiency of a nozzle and performance of a cycle. Most of the researches on shock waves deal with their occurrence in flows of condensing steam at high quality. Both experimental (Moore et al., 1973) and numerical (Simpson and White, 2005; Kermali and Gerber, 2003) investigations revealed aerodynamic shock wave which has supersonic flow at its back. This result is different from the findings in our series of studies, wherein shock wave with subsonic flow at its back was obtained experimentally for supersonic two-phase flow of CO_2 from low to medium quality.

In our first previous studies, non-equilibrium shock waves were modeled (Nakagawa et al., 2006) and their occurrence along the diverging sections of relatively long nozzles were investigated in a blowdown device (Berana, 2005). The following dimensional parameters are the same for the nozzles: thickness of 3 mm, total length of 82 mm divided into 25.85-mm segment for the converging section and 56.15-mm segment for the diverging section. The converging section has an inlet height of 10 mm and the throat has a height of 0.24 mm. The divergence angles used were 0.306° (Long Nozzle 1) and 0.612° (Long Nozzle 2). Inlet conditions were selected near the critical point, wherein the pressure range was 8–9 MPa and the obtained temperature range was 25–41°C. Correspondingly, back pressures ranged from 1.2 to 4.2 MPa. Such undertaking led to the analysis of experimentally obtained shock waves at almost the same inlet conditions with respect to divergence angle. In the second study (Berana, 2009; Berana et al., 2009; Nakagawa et al., 2008), the converging section had a 10 mm inlet height and a 15-mm length (Short Nozzle). It has 0.24-mm throat height and 1-mm plate thickness. The simulated length based on Isentropic Homogeneous Equilibrium model and corresponding to a common 9.5-MPa condenser outlet at 40°C and 3.5-MPa evaporator pressure was 8.38 mm. The corresponding divergence angle was 0.48°. The refrigeration cycle used was a modified simple vapor compression cycle with a compressor output power of 1.3 kW. The expansion valve was replaced by a converging-diverging nozzle to isolate it and to easily investigate its inlet and the outlet states. The inlet conditions used were 9–11 MPa at 37–55°C. To determine different intensities of shock waves, the widest possible back-pressure range obtained was 3.6–5.9 MPa. Experimental results showed that shock waves intensity depends on supercritical inlet condition.

This paper used the theoretical model for nonequilibrium flow and shock waves in our previous studies (Nakagawa et al., 2006) to simulate the behavior of shock waves with varying divergence angle and supercritical inlet conditions. The presented simulation results in this paper were found to be in agreement with our experimental findings in two-phase flow of CO_2 in converging-diverging nozzles. Most of this study was initially presented in the 10th International Institute of Refrigeration – Gustav Lorentzen Conference on Natural Working Fluids (IIR-GL) at Delft, The Netherlands (Berana and Nakagawa, 2012). The current paper experimentally validates the introduced flow model; and the applicability of the study to the ejector refrigeration system is emphasized.

2. NONEQUILIBRIUM FLOW AND NONEQUILIBRIUM SHOCK WAVES: GOVERNING EQUATIONS INCORPORATING MOMENTUM AND THERMAL NON-EQUILIBRIA

The governing equations of shock waves in the vapor-droplet flow in a nozzle shown in Fig. 1 are presented in this section. This formulation was adopted from our previous study (Nakagawa et al., 2006). Flow of uniformly dispersed droplets and vapor was assumed. Inter-phase transfers between the phases that include mass, momentum and heat as illustrated in Fig. 2 were considered. Momentum and thermal relaxation phenomena were incorporated in those equations which could be applicable to two-phase flow of any working fluid. Results of simulation using the equations as compared to the results of experiment for supersonic two-phase flow of CO_2 in converging-diverging nozzles intended for ejector refrigeration systems are shown in this paper.

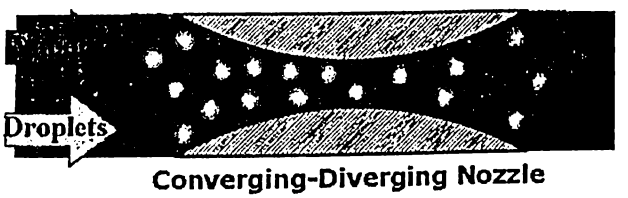

Figure 1. One-dimensional vapor-droplet flow

Figure 2. Inter-phase transfers

Two-phase flow through a converging-diverging nozzle was also modeled as a steady-state steady-flow process. The flow was also assumed to be one-dimensional and parallel to the nozzle's centerline z which is normal to any arbitrary flow cross section. Anywhere in the flow, either phase can be changed to the other by condensation or evaporation as also illustrated in Fig. 2. This means that x varies with z.

The droplet, droplet surface and vapor phase were considered to have different temperatures. The pressure of the droplet surface was used in the calculation. The effect of surface tension was not considered in the calculation because the pressure difference between the core and surface of a droplet was found to be negligible. The calculated values of that pressure difference ranged only from 0.03 to 2 kPa. The surface is assumed to only transfer heat but not momentum.

2.1 Conservation of Mass

The equation for conservation of mass was differentiated with respect to the flow direction z, and the specific volumes of droplets and vapour phases were partially differentiated with respect to pressure and temperatures of vapour and liquid. The derived equation is

$$-\frac{x}{\rho_g u_g^2}\frac{du_g}{dz}-\frac{1-x}{\rho_l u_l^2}\frac{du_l}{dz}+\left[\frac{x}{u_g}\left(\frac{\partial v_g}{\partial P}\right)_{T_g}+\frac{1-x}{u_l}\left(\frac{\partial v_l}{\partial P}\right)_{T_l}\right]\frac{dP}{dz}+\left(\frac{1}{\rho_g u_g}-\frac{1}{\rho_l u_l}\right)\frac{dx}{dz} \quad (1)$$
$$+\frac{x}{u_g}\left(\frac{\partial v_g}{\partial T_g}\right)_P\frac{dT_g}{dz}+\frac{1-x}{u_l}\left(\frac{\partial v_l}{\partial T_l}\right)_P\frac{dT_l}{dz}=\frac{1}{W}\frac{dA}{dz}$$

2.2 Conservation of Energy

The basic equation for conservation of energy was differentiated along the flow axis, and differentials of enthalpies along the same axis with respect to pressure and temperatures of droplet and vapor were substituted. The resulting equation is

$$xu_g\frac{du_g}{dz}+(1-x)u_l\frac{du_l}{dz}+\left[x\left(\frac{\partial h_g}{\partial P}\right)_{T_g}+(1-x)\left(\frac{\partial h_l}{\partial P}\right)_{T_l}\right]\frac{dP}{dz} \quad (2)$$
$$+\left(\frac{u_g^2}{2}-\frac{u_l^2}{2}+h_{gl}\right)\frac{dx}{dz}+x\left(\frac{\partial h_g}{\partial T_g}\right)_P\frac{dT_g}{dz}+(1-x)\left(\frac{\partial h_l}{\partial T_l}\right)_P\frac{dT_l}{dz}=0$$

2.3 Conservation of Momentum

The momentum equation of two-phase flow in the form of pressure drop with negligible friction is shown by

$$\frac{d}{dz}\left[xu_g+(1-x)u_l\right]=-\frac{A}{W}\frac{dP}{dz} \quad (3)$$

2.4 Momentum Relaxation between Droplets and Vapor

The equation of motion of a droplet was formulated by incorporating Stokes' frictional drag, and the derived expression containing momentum relaxation between droplets and vapor is

$$\frac{du_l}{dz}+\frac{1}{u_l\rho_l}\frac{dP}{dz}=\frac{u_g-u_l}{u_l\tau_m} \quad (4)$$

Where, the momentum relaxation time required for both phases to reach dynamic equilibrium is

$$\tau_m = \frac{\rho_l d^2}{18\mu_g} \tag{5}$$

2.5 Thermal Relaxation of Vapor

When condensation or evaporation occurs, the latent heat of phase change transfers between the phases and causes an increase or decrease in entropy of each phase. By using the governing equation for heat transfer between the surface of droplet and vapor, the derived expression containing thermal relaxation between surface of droplets and vapor is

$$u_g \frac{dT_g}{dz} = \frac{1-x}{x}\frac{\rho_g}{\rho_l}\frac{T_s - T_g}{\tau_{Tg}} - \left(\frac{\partial s_g}{\partial P}\right)_{T_s}\frac{T_g u_g}{c_{Pg}}\frac{dP}{dz} \tag{6}$$

Where, the thermal relaxation time of vapor, which is the time required for the surface and the vapor to reach thermal equilibrium, is given by

$$\tau_{Tg} = \frac{\rho_g c_{Pg} d}{6\alpha_g} \tag{7}$$

2.6 Thermal Relaxation of Droplets

In relation to the previous subsection, by using the equation of surface-to-droplet heat transfer, the derived expression containing thermal relaxation between a droplet and its surface is

$$u_l \frac{dT_l}{dz} = \frac{T_s - T_l}{\tau_{Tl}} - \left(\frac{\partial s_l}{\partial P}\right)_T \frac{T_l u_l}{c_{Pl}}\frac{dP}{dz} \tag{8}$$

Likewise, the thermal relaxation time of a droplet, which is the time required for the surface and the droplet to reach thermal equilibrium, is given by

$$\tau_{Tl} = \frac{\rho_l c_{Pl} d}{6\alpha_l} \tag{9}$$

2.7 Equation of the Saturated Line (Clausius-Clapeyron Equation)

It was assumed that heat transfer is only affected by evaporation and condensation. For this case, the equation of the saturated line known as the Clausius-Clapeyron equation (Moran and Shapiro, 2004) was included in the governing equations. The equation was differentiated along the z axis and the resulting equation for formulation is

$$\frac{dP}{dz} - \frac{h_g - h_l}{T_s\left(\frac{1}{\rho_g} - \frac{1}{\rho_l}\right)}\frac{dT_s}{dz} = 0 \tag{10}$$

2.8 Solution Method

The governing equations were set in the simulation, forming linear differential equations. The values of the differential variables were obtained using Gaussian elimination. The differential variables were integrated step by step using Runge-Kutta method to solve the variables along the flow axis.

The simulation is only limited to the two-phase region of CO_2 (Fig. 3). The start of phase change was used as the initial condition and a successful calculation ended at the outlet. The start of calculation was limited at the inlet instead of the throat.

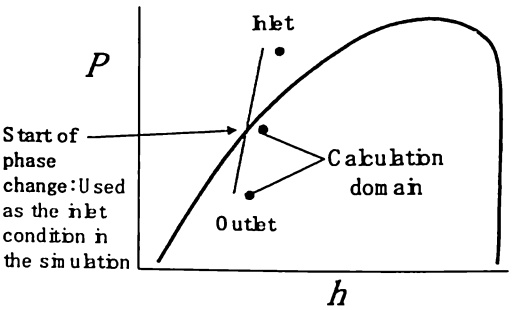

Figure 3. Simulation process

3. RESULTS AND DISCUSSIONS

The results of simulation are shown in Fig. 4a and 4b for Long Nozzle 1 and 2, respectively, and in Fig. 4c and 4d for Short Nozzle at saturated inlet conditions of 29°C at a quality of 0.001 and of 26°C at a quality of 0.999, respectively. The inlet condition had to be above the saturated line or even in the supercritical region just like the inlet conditions in the experiment. However, starting there required that complicated problems of initiation of liquid breakup or nucleation have to be considered. The slightly saturated state in each simulation run was chosen as the inlet condition to avoid the problems because the focus of this study was only to observe the shock waves in the diverging section. Two-phase flow was assumed to occur in the entire nozzle. The intersection of the isentropic flow for each run with the saturated line was used to obtain the initial saturated temperature. The isentropic flow started from the inlet condition defined by measured pressure and temperature of the corresponding experiment run. The initial saturated temperature and an adjusted quality, which could either be 0.001 for slightly saturated liquid or 0.999 for slightly saturated vapor, were used as the inlet condition for a simulation run to approximate two-phase behavior. The decompression profiles in the diverging sections from the simulation which considered slightly saturated conditions at the inlets of the nozzles are in good agreement with the decompression profiles in the diverging sections from the experiments as shown in Figs. 4 and 5. This means that the non-equilibrium model for two-phase flow and shock waves can predict the characteristics of two-phase flow and shock waves for the flow conditions and nozzle dimensions considered in this study. The inlet mass flow rates for all nozzles were calculated by assigning a fixed value of the outlet pressure which was lower than the inlet pressure as referred to the experiment data.

Supersonic characteristics and two-phase shock waves appeared in cases where the critical mass flow rates in the nozzles were exceeded. The calculated frozen Mach number contradicted with the calculated equilibrium Mach number. The former value was less than unity but the latter was greater than unity for the whole diverging section. At the throat, a sound speed of about 300 m/s was obtained for frozen flow. It was nearly equal to the sound speed of the vapor phase. Conversely, a sound speed of about 100 m/s was obtained for equilibrium flow. The computed velocity at the throat was about 150 m/s from the experiment data.

While the frozen Mach number which was governed by the basic equations was still less than unity, the outlet pressure was adjusted by slightly changing the inlet mass flow rates. Simultaneously, the produced shock wave moved downstream and the outlet pressure decreased. To illustrate the calculation, the new profiles obtained by slightly increasing the mass flow rates, which means decreasing the pressure, were plotted using dashed curves in Fig. 4. Intermediate conditions between frozen and equilibrium flows, and the initial ratios of the outlet pressures to the inlet pressures based on experiment were used to compare the calculated data to the experimentally obtained ones.

The flows were subsonic based on the frozen Mach numbers. From mathematical standpoint, the mass flow rates were not at their critical values yet because they could still be increased even by small increments. This meant that choked or supersonic flows were not happening yet. On the contrary, the flows were supersonic based on the equilibrium Mach numbers. From engineering standpoint, the mass flow rates were considered to be constant because the increments obtained were very small. The flow rates were assumed to be the critical flow rates and the flows could be described as supersonic. To determine the exact condition ranging from frozen to equilibrium flow, the corresponding relaxation times which indicated the transport phenomena in two-phase flow had to be determined. The relaxation times were functions of the droplet diameter as indicated by Eqn. 5, 7 and 9. The droplet diameter however, had no other equation which is independent of the relaxation times. Therefore, there was no other way to calculate the relaxation times. Its experimental values were not determined also because the droplet diameters were not measured in the experiment. Because there are still no published data on measured droplet diameters of supersonic two-phase flow of CO_2 in converging-diverging nozzles to the best of our knowledge, the values for wet steam flow which are in the order of 10 μm as determined in previous experiments in our laboratory and in the experiment of Comfort et al. (1978) were used.

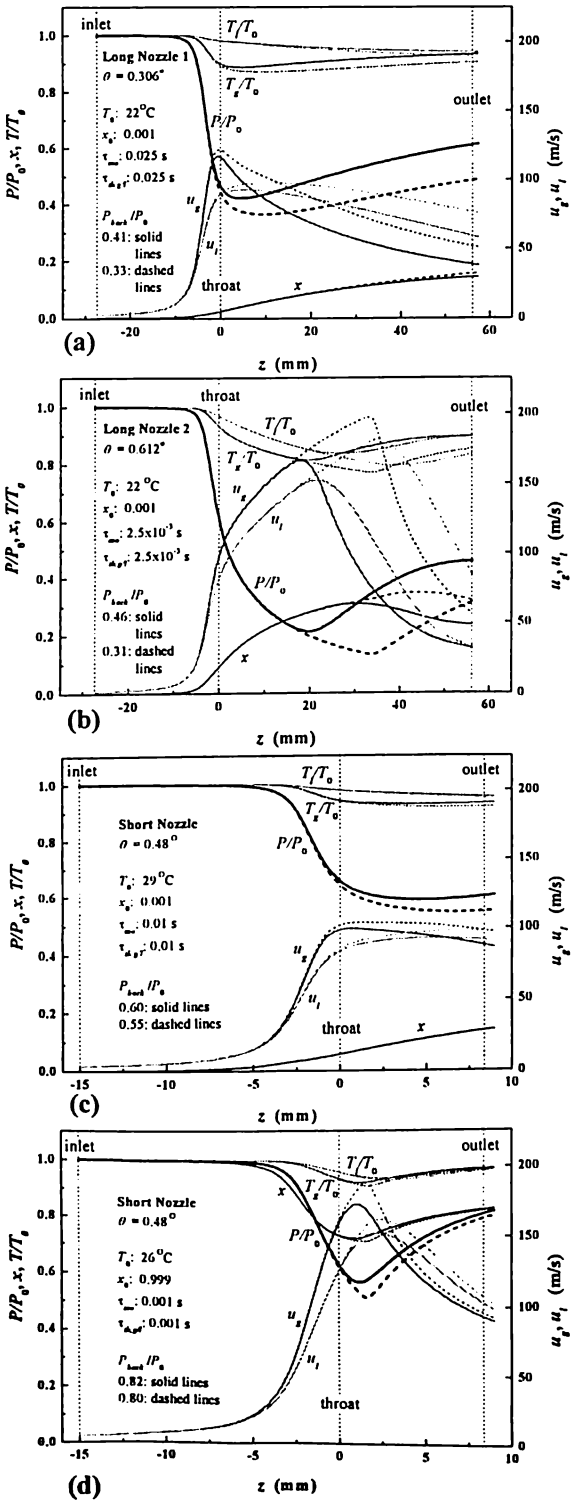

Figure 4. Simulated shock

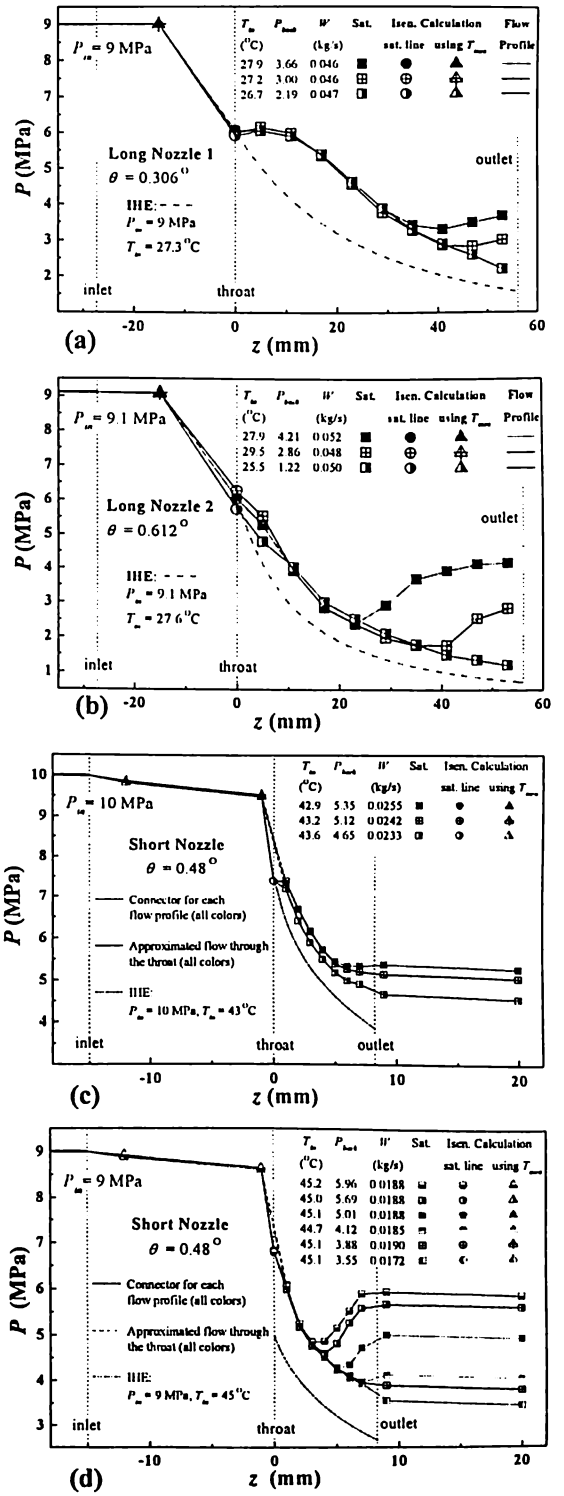

Figure 5. Shock waves from

Experimental relaxation times were predicted by choosing droplet diameters in the range of 10–120 μm and using the measured two-phase flow temperatures and the momentum relaxation time given in Eqn. 5. For simplicity, all relaxation times were set as equal, but the momentum equation was used because nonequilibrium in momentum is more dominant than thermal nonequilibrium as has been established in many studies. The assigned diameters of droplets were used just for making initial analysis of nonequilibrium two-phase flow and shock waves with respect to relaxation times.

Relaxation times were iteratively predicted until the theoretical pressure profiles of shock waves matched with the experimental ones. The resulting shock waves were analyzed according to their strength and relaxation characteristics.

3.1 Pseudo-shock Waves and Dispersed Shock Waves Determined from the Simulation and in Agreement with Experimental Results

The simulated pseudo shock waves shown in Fig. 4a and 4c matched with the experimentally obtained profiles for Long Nozzle 1 shown in Fig. 5a and for Short Nozzle shown in Fig. 5c. The profiles indicated that gradual phase change occurred and large droplets, which were estimated to be around 60–110 μm in diameter, were created. The relaxation times τ_m, τ_{Tg}, and τ_{Tl} were found to be 0.025 second for Long Nozzle 1 and 0.01 second for the Short Nozzle. The increase in pressure of the shock waves was small. The behavior was a condition away from equilibrium because almost no interaction between the two phases along the diverging section was observed. The quality has only a gradual slope which indicated slow phase change.

The velocities and temperatures of both phases also have gradual slopes which indicated weak interaction between the phases. The condition was approaching the behavior of frozen flow even if the relaxation times were still near to the relaxation time of equilibrium flow which is zero. This condition indicates that the large droplets formed could not be easily slowed down by the vapor in the diverging section because of their large inertia. Pseudo-shock waves, in agreement with the experimental results (Berana, 2009; Berana et al., 2009; Nakagawa et al., 2008) and similar simulation results (Nakagawa et al., 2006) of our previous studies, were also predicted.

The simulated dispersed shock waves shown in Fig. 4b and 4d matched with the experimentally obtained profiles for Long Nozzle 2 shown in Fig. 5b and for Short Nozzle shown in Fig. 5c. Significantly lower values of 0.0025 second for Long Nozzle 2 and 0.001 second for the Short Nozzle were obtained for the relaxation times. Droplets with diameters around 20–40 μm, which were smaller than those of Long Nozzle 1 and Short Nozzle at an inlet quality of 0.001, were created. The behavior was a near-equilibrium condition and characterized by shorter relaxation times that are very close to zero. A significant interaction between the two phases along the diverging section was observed. The quality has a steeper slope which indicated faster phase change than that of pseudo-shock waves. The velocities and temperatures of both phases also have steeper slopes which indicated relatively strong interaction between the phases. This condition indicates that the small droplets formed could be easily slowed down by the vapor in the diverging section because of their small inertia. Dispersed shock waves, as experimentally determined and simulated in our previous studies mentioned, were also predicted in this case.

3.2 Shock Waves Behavior under the Same Inlet Condition but Different Divergence Angles

The variation of relaxation times with respect to divergence angle was determined from the simulation results in Fig. 4a and 4b and verified by the experiment results in Fig. 5a and 5b. The relaxation times decreased while shock waves intensified with increasing divergence angle.

3.3 Shock Waves Behavior in the Same Nozzle but Different Inlet Conditions

Simulation also showed increasing intensity of shock waves with increasing supercritical inlet entropy. The shock waves got stronger while the relaxation times decreased with increasing supercritical inlet entropy as indicated by the increase in inlet quality from 0.001 in Fig. 4c to 0.999 in Fig. 4d. This behavior is verified by the results in Fig. 5c for pseudo-shock waves and in Figure 5d for dispersed shock waves.

4. CONCLUSIONS

Weak pseudo-shock waves and dispersed shock waves associated with relaxation phenomena appeared in the simulation of this study. Weak pseudo-shock waves occurred in liquid-dominated two-phase flow, while relatively stronger dispersed shock waves occurred in vapor-dominated flow. It was simulated and verified in this study that shock waves intensify with increasing divergence angle given the same inlet condition, and with increasing supercritical inlet entropy given the same nozzle. The results are in agreement with the experiment and similar simulation results in our previous studies.

ACKNOWLEDGEMENTS

The authors would like to sincerely thank Japan International Cooperation Agency (JICA) for the scholarship fund in Toyohashi University of Technology during the course of this research. Dr. Berana is also giving sincere appreciation to the Engineering Research and Development for Technology (ERDT) Program of the republic of the Philippines for the research dissemination fund.

NOMENCLATURE

A	cross-sectional area of flow (m^2)
c	specific heat (J/kg-K)
d	droplet diameter (m)
h	enthalpy (J/kg)
P	pressure (Pa)
s	entropy (J/kg-K)
T	temperature (°C, K)
u	velocity (m/s)
W	mass flow rate (kg/s)
x	quality
z	one-dimensional flow axis

Greek Letters

α	thermal conductivity (W/m-K)
μ	viscocity (Pa-s)
v	specific volume (m^3/kg)
ρ	density (kg/m3)
τ	relaxation time(s)

Subscripts

g	vapour phase
gl	difference from vapour to liquid phases
l	liquid phase
m	momentum
P	constant pressure
s	surface, saturated
T	constant temperature, thermal

REFERENCES

1. Berana, M.S., 2005. Characteristics of Supersonic Two-phase Flow of Carbon Dioxide through a Converging-diverging Nozzle of an Ejector Used in a Refrigeration Cycle, Master's Thesis, Toyohashi University of Technology, Toyohashi, Aichi, Japan.
2. Berana, M.S., 2009. Characteristics and Shock Waves of Supersonic Two-phase Flow of CO_2 through Converging-diverging Nozzles, Doctoral Dissertation, Toyohashi University of Technology, Toyohashi, Aichi, Japan.
3. Berana, M.S., Nakagawa, M., 2012. Simulation of Shock Waves in Supersonic Flow of CO_2 through a Converging-Diverging Nozzle of Transcritical Ejector Refrigeration System. Proceedings of the 10th International Institute of Refrigeration – Gustav Lorentzen Conference on Natural Working Fluids (IIR – GL), Delft, The Netherlands, June 25-27, 2012, 288:1–8.
4. Berana, M.S., Nakagawa, M., Harada, A., 2009. Shock waves in supersonic two-phase flow of CO_2 in converging-diverging nozzles. HVAC&R Research 15(6), 1065–1079.
5. Comfort, W.J. III, Alger, T.W., Giedt, W.H., Crowe, C.T., 1978. Calculation of two-phase dispersed droplet-in-vapor flows including normal shock waves. Journal of Fluids Engineering: ASME Transactions 100, 355–362.
6. Kermani, M.J., Gerber, A.G., 2003. A general formula for the evaluation of thermodynamic and aerodynamic losses in nucleating steam flow. International Journal of Heat and Mass Transfer 46, 3265–3278.
7. Moran, M.J., Shapiro, H.N., 2004. Fundamentals of Engineering Thermodynamics, fifth edn. John Wiley & Sons, Hoboken, NJ. pp. 141–147.
8. Moore, M.J., Walters P.T., Crane R.I., Davidson B.J., 1973. Predicting the fog-drop size in wet-steam turbines. Wet Steam 4, Conference Publication of the Institute of Mechanical Engineers, University of Warwick, UK, Paper No. C37/73, pp. 101–109.
9. Nakagawa, M., Berana, M.S., and Harada, A., 2008. Shock waves in supersonic two-phase flow of CO_2 in converging-diverging nozzles. Proceedings of the 12th International Refrigeration and Air Conditioning Conference at Purdue, West Lafayette, IN, USA, July 14-17, 2008, 2165:1–8.
10. Nakagawa, M., Takeuchi, H., Berana, M.S., 2006. Supersonic characteristics and shock waves in two-phase flow along a nozzle of a carbon dioxide ejector. Proceedings of the 3rd Asian Conference on Refrigeration and Air-conditioning (ACRA 2006), Gyeongju, South Korea, May 21-23, 2006, 1: 363–367.
11. Simpson, D.A., White, A.J., 2005. Viscous and unsteady flow calculations of condensing steam in nozzles. International Journal of Heat and Fluid Flow 26, 71–79.